Lanthanide(III)/Actinide(III) Differentiation in the Cerium and Uranium Complexes [M(C$_5$Me$_5$)$_2$(L)]$^{0,+}$ (L = 2,2′-Bipyridine, 2,2′:6′,2″-Terpyridine): Structural, Magnetic, and Reactivity Studies

Thouraya Mehdoui,[a] Jean-Claude Berthet,*[a] Pierre Thuéry,[a] Lionel Salmon,[a] Eric Rivière,[b] and Michel Ephritikhine*[a]

Abstract: Treatment of [Ce(Cp*)$_2$I] or [U(Cp*)$_2$I(py)] with 1 mol equivalent of bipy (Cp* = C$_5$Me$_5$; bipy = 2,2′-bipyridine) in THF gave the adducts [M-(Cp*)$_2$I(bipy)] (M = Ce (**1a**), M = U (**1b**)), which were transformed into [M-(Cp*)$_2$(bipy)] (M = Ce (**2a**), M = U (**2b**)) by Na(Hg) reduction. The crystal structures of **1a** and **1b** show, by comparing the U−N and Ce−N distances and the variations in the C−C and C−N bond lengths within the bidentate ligand, that the extent of donation of electron density into the LUMO of bipy is more important in the actinide than in the lanthanide compound. Reaction of [Ce(Cp*)$_2$I] or [U(Cp*)$_2$I(py)] with 1 mol equivalent of terpy (terpy = 2,2′:6′,2″-terpyridine) in THF afforded the adducts [M(Cp*)$_2$(terpy)]I (M = Ce (**3a**), M = U (**3b**)), which were reduced to the neutral complexes [M(Cp*)$_2$-(terpy)] (M = Ce (**4a**), M = U (**4b**)) by sodium amalgam. The complexes [M-(Cp*)$_2$(terpy)][M(Cp*)$_2$I$_2$] (M = Ce (**5a**), M = U (**5b**)) were prepared from a 2:1 mixture of [M(Cp*)$_2$I] and terpy. The rapid and reversible electron-transfer reactions between **3** and **4** in solution were revealed by ^{1}H NMR spectroscopy. The spectrum of **5b** is identical to that of the 1:1 mixture of [U(Cp*)$_2$I(py)] and **3b**, or [U(Cp*)$_2$I$_2$] and **4b**. The magnetic data for **3** and **4** are consistent with trivalent cerium and uranium species, with the formulation [M^{III}(Cp*)$_2$(terpy$^{·-}$)] for **4a** and **4b**, in which spins on the individual units are uncoupled at 300 K and antiferromagnetically coupled at low temperature. Comparison of the crystal structures of **3b**, **4b**, and **5b** with those of **3a** and the previously reported ytterbium complex [Yb(Cp*)$_2$(terpy)] shows that the U−N distances are much shorter, by 0.2 Å, than those expected from a purely ionic bonding model. This difference should reflect the presence of stronger electron transfer between the metal and the terpy ligand in the actinide compounds. This feature is also supported by the small but systematic structural variations within the terdentate ligands, which strongly suggest that the LUMO of terpy is more filled in the actinide than in the lanthanide complexes and that the canonical forms [U^{IV}(Cp*)$_2$-(terpy$^{·-}$)]I and [U^{IV}(Cp*)$_2$(terpy^{2-})] contribute significantly to the true structures of **3b** and **4b**, respectively. This assumption was confirmed by the reactions of complexes **3** and **4** with the H$^·$ and H$^+$ donor reagents Ph$_3$SnH and NEt$_3$HBPh$_4$, which led to clear differentiation of the cerium and uranium complexes. No reaction was observed between **3a** and Ph$_3$SnH, while the uranium counterpart **3b** was transformed in pyridine into the uranium(IV) compound [U(Cp*)$_2${NC$_5$H$_4$(py)$_2$}]I (**6**), where NC$_5$H$_4$(py)$_2$ is the 2,6-dipyridyl-(hydro-4-pyridyl) ligand. Complex **6** was further hydrogenated to [U(Cp*)$_2$-{NC$_5$H$_8$(py)$_2$}]I (**7**) by an excess of Ph$_3$SnH in refluxing pyridine. Treatment of **4a** with NEt$_3$HBPh$_4$ led to oxidation of the terpy$^{·-}$ ligand and formation of [Ce(Cp*)$_2$(terpy)]BPh$_4$, whereas similar reaction with **4b** afforded [U-(Cp*)$_2${NC$_5$H$_4$(py)$_2$}]BPh$_4$ (**6′**). The crystal structures of **6**, **6′** and **7** were determined.

Keywords: cerium · electron transfer · magnetic properties · N ligands · uranium

[a] T. Mehdoui, Dr. J.-C. Berthet, Dr. P. Thuéry, Dr. L. Salmon, Dr. M. Ephritikhine
Service de Chimie Moléculaire
Bât. 125, DSM, DRECAM, CNRS URA 331, CEA/Saclay
91191 Gif-sur-Yvette (France)
Fax: (+33) 1-69-08-66-40
E-mail: berthet@drecam.cea.fr
        ephri@drecam.cea.fr

[b] Dr. E. Rivière
Laboratoire de Chimie Inorganique
Institut de Chimie Moléculaire et des Matériaux
CNRS UMR 8613, Université de Paris-Sud
91405 Orsay Cedex (France)

Introduction

Discrimination between trivalent lanthanide (Ln) and actinide (An) compounds with polydentate N-heterocyclic bases is an important problem for both its fundamental aspects, that is, precise knowledge of the metal–ligand bonds and the respective roles of the 4f and 5f electrons,[1] and its applications, particularly in the management of nuclear wastes.[2]

Lanthanide complexes with polydentate nitrogen ligands have already been reported,[1c,3–8] in particular the 2,2′-bipyridine (bipy) and 1,10-phenanthroline (phen) and 2,2′:6′,2″-terpyridine (terpy) adducts of bis(pentamethylcyclopentadienyl)lanthanides [Ln(Cp*)$_2$(bipy)] and [Ln(Cp*)$_2$(phen)] (Cp* = C$_5$Me$_5$; Ln = Sm or Yb)[9–11] and [Yb(Cp*)$_2$(terpy)].[12] These compounds have the formal appearance of divalent lanthanide compounds but are in fact Ln^{III} complexes with a ligand radical anion. In addition to their structural and physicochemical properties, such species are attractive for their reactivity, since they are considered to be synthetic equivalents of low-valent species.[13] Such 5f element complexes with azine ligands seem to have been neglected since the reports of the uranium bipyridine compounds [U(bipy)$_4$][14] and [U(COT)(Cp*)(Me$_2$bipy)] (COT = η-C$_8$H$_8$, Me$_2$bipy = 4,4′-dimethyl-2,2′-bipyridine),[15] in which the metal oxidation state is questionable. Following our studies on the differentiation of trivalent lanthanide and uranium ions, especially those concerning the coordination of azine molecules to tris(cyclopentadienyl) complexes of cerium and uranium[16,17] and the selective complexation of uranium(III) over lanthanide(III) triflates or iodides by bipy,[3] phen[18] and terpy,[4–6] we speculated that the distinct electronic behavior of the 4f and 5f ions, in particular the easier oxidation and better π-donating ability of the actinide, should emerge and lead to significant differences in the structures and reactions of the electron-rich complexes [Ce(Cp*)$_2$(L)]$^{n+}$ and [U-(Cp*)$_2$(L)]$^{n+}$ (L = bipy, phen, terpy; n = 1, 0). Here we report on the synthesis and structural and chemical characterization of the bipyridine compounds [M(Cp*)$_2$I(bipy)] and [M(Cp*)$_2$(bipy)] (M = Ce, U) and the terpyridine complexes [M(Cp*)$_2$(terpy)]$^{n+}$ (M = Ce, U; n = 1, 0). The uranium complexes [U(Cp*)$_2$(bipy)] and [U(Cp*)$_2$(terpy)] permitted a new approach to comparing the properties of low-valent lanthanide (Ln) and actinide (An) complexes.

Results and Discussion

Synthesis, crystal structures and reduction of [M(Cp*)$_2$I-(bipy)] (M = Ce, U): Reaction of [Ce(Cp*)$_2$I] or [U-(Cp*)$_2$I(py)] with 1 mol equivalent of bipy in THF readily gave the adducts [M(Cp*)$_2$I(bipy)] [M = Ce (**1a**), M = U (**1b**); Eq. (1)]; after evaporation of the solvent and washing with diethyl ether, **1a** and **1b** were isolated as analytically pure orange and black powders in 81 and 72% yield, respectively. Crystals of **1a** and **1b** were obtained by slow diffusion of pentane or diethyl ether, respectively, into a THF solution.

$$[M(Cp^*)_2I] + bipy \rightarrow [M(Cp^*)_2I(bipy)]$$
$$M = Ce \ (\mathbf{1a}) \qquad\qquad (1)$$
$$M = U \ (\mathbf{1b})$$
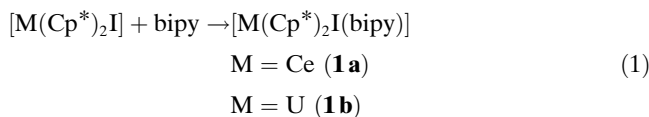
The crystal structures of **1a** and **1b** are very similar; a view of the cerium complex **1a** is shown in Figure 1. The complex adopts the relatively common bent-sandwich
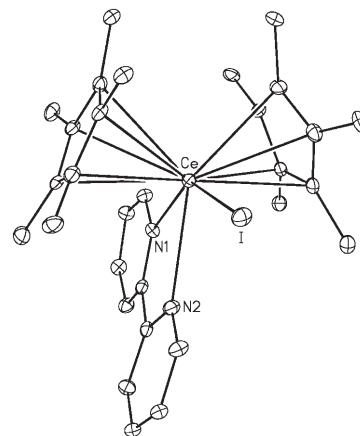

Figure 1. Crystal structure of [Ce(Cp*)$_2$I(bipy)] (**1a**) with thermal ellipsoids drawn at the 20% probability level. H atoms have been omitted. Selected bond lengths [Å] and angles [°]; the corresponding values in the uranium analogue **1b** are given in brackets: ⟨Ce−C⟩ 2.83(3) [2.82(3)], Ce−I 3.2048(7) [3.2135(4)], Ce−N1 2.633(6) [2.635(5)], Ce−N2 2.782(6) [2.561(4)]; N1-Ce-N2 60.07(19) [62.39(15)].

M(Cp*)$_2$X$_2$Y configuration with the bipy and iodide ligands in the equatorial girdle.[19] The average Ce−N and U−N distances of 2.71(7) and 2.60(4) Å can be compared with those of 2.67(3) and 2.65(4) Å in [MI$_3$(bipy)$_2$(py)] (M = Ce, U), the only other pair of analogous Ln^{III} and U^{III} complexes with bipy ligands to have been crystallographically characterized;[3] the difference of 0.11 Å between the mean Ce−N and U−N bond lengths in **1a** and **1b** is much larger than that of 0.02 Å in [MI$_3$(bipy)$_2$(py)] (M = Ce, U) and [M-(C$_5$H$_4$R)$_3$(L)] (M = Ce, U; R = Me$_3$Si, tBu; L = azine).[16] The shortening of the U−N distances with respect to the Ce−N distances in analogous cerium(III) and uranium(III) complexes with aromatic nitrogen bases, although the ionic radius of the U^{III} ion is 0.01 Å larger than that of Ce^{III},[20] was related to the greater strength of the U−N bonds and the greater stability of the uranium complexes, and was accounted for by electron transfer between the uranium atom and the terpy ligand, which is less likely in the lanthanide counterpart.

The extent of donation of electron density into the LUMO of the bipyridine ligand in various complexes, in particular [Yb(Cp*)$_2$(bipy)]$^+$ and [Yb(Cp*)$_2$(bipy)], was assessed from the systematic changes in the bond lengths in the bidentate molecule.[10,21,22] The C−C and C−N bond lengths of the bipy ligands in **1a** and **1b** are listed in Table 1; these values can be compared with those of free

Table 1. Comparison of averaged C–C and C–N bond lengths [Å] in the bidentate ligands.

Bond	bipy[22]	[Yb(Cp*)$_2$(bipy)]$^{+}$ [10]	[Ln(Cp*)$_2$(bipy)] (Ln = Yb;[10] Sm[9])	[Ce(Cp*)$_2$(bipy)]I (1a)[a]	[U(Cp*)$_2$(bipy)]I (1b)[a]
A	1.490(3)	1.492	1.434; 1.43	1.494	1.474
B	1.394(2)	1.385	1.419; 1.42	1.383(1)	1.389(6)
C	1.385(2)	1.380	1.387; 1.34	1.379(8)	1.376(6)
D	1.383(2)	1.370	1.420; 1.41	1.374(1)	1.384(11)
E	1.384(2)	1.370	1.398; 1.37	1.381(3)	1.369(2)
F	1.341(2)	1.339	1.358; 1.35	1.340(2)	1.356(1)
G	1.346(2)	1.343	1.383; 1.38	1.357(2)	1.364(1)

[a] Standard deviations of averaged values are given in parenthesis.

transoid bipy,[22] chelating bipy in [Yb(Cp*)$_2$(bipy)]$^{+}$[10] and the radical anion bipy$^{\cdot-}$ in [Ln(Cp*)$_2$(bipy)] (Ln = Sm,[9] or Yb[10]). The distances A–G in **1a** correspond effectively to a neutral bipy ligand, but comparison of these distances with those in **1b** seems to reveal that bonds A and E are shortened, while bonds B, D, F and G are lengthened in the uranium complex, albeit with little statistical significance; this trend is precisely that expected from the acceptance of electron density into the LUMO of bipy.[10,21,22]

Reduction of **1a** and **1b** with sodium amalgam in THF led to formation of the compounds [M(Cp*)$_2$(bipy)] [M=Ce (**2a**), M=U (**2b**); Eq. (2)]. After evaporation of the solvent and extraction with toluene, uranium complex **2b** was isolated as a dark green powder in 80 % yield; the cerium analogue **2a** was characterized only by its ^{1}H NMR spectrum.

$$[M(Cp^*)_2I(bipy)] + Na(Hg) \rightarrow [M(Cp^*)_2(bipy)] + NaI$$
$$M = Ce \ (\mathbf{2a}) \quad\quad (2)$$
$$M = U \ (\mathbf{2b})$$
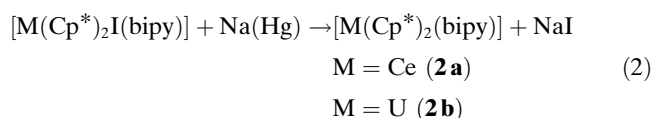
By analogy with the [Ln(Cp*)$_2$(bipy)] congeners (Ln = Sm, Yb), these compounds should be formulated as [M^{III}-
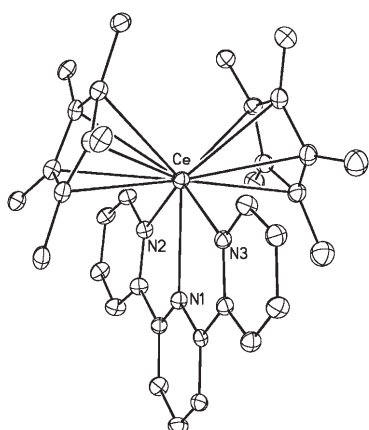

Figure 2. Crystal structure of the cation in [Ce(Cp*)$_2$(terpy)]I (**3a**) with thermal ellipsoids drawn at the 10 % probability level. H atoms have been omitted.

(Cp*)$_2$(bipy$^{\cdot-}$)]; the presence of the radical anion bipy$^{\cdot-}$ is moreover confirmed by the large chemical shifts of the ^{1}H NMR signals, which for **2a** range from $\delta = -26.91$ to -253.11, while those of **1a** range from $\delta = 8.94$ to -32.5.

Synthesis and crystal structures of [M(Cp*)$_2$(terpy)]I and [M-(Cp*)$_2$(terpy)] (M = Ce, U): Treatment of [Ce(Cp*)$_2$I] with 1 mol equivalent of terpy in THF led to formation of the cationic complex [Ce(Cp*)$_2$-(terpy)]I [**3a**; Eq. (3)]; orange crystals of the solvate **3a**·THF deposited on cooling the solution and were isolated in 72 % yield. Similar reaction of [U(Cp*)$_2$I(py)] with terpy afforded, after evaporation of the solvent, a black powder of the uranium analogue [U(Cp*)$_2$(terpy)]I (**3b**) in 90 % yield; black crystals of **3b**·THF were formed upon slow diffusion of diethyl ether into THF.

$$[M(Cp^*)_2I] + terpy \rightarrow [M(Cp^*)_2(terpy)]I$$
$$M = Ce \ (\mathbf{3a}) \quad\quad (3)$$
$$M = U \ (\mathbf{3b})$$
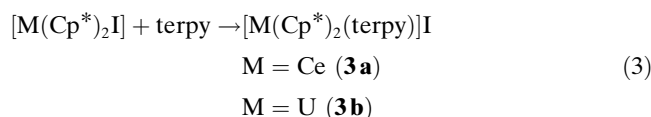
The crystals of **3a**·THF and **3b**·THF are composed of discrete cation–anion pairs and THF molecules. The cations adopt the same bent sandwich configuration as **1a** and **1b** with the terdentate ligand in the equatorial girdle. A view of the cerium cation is shown in Figure 2, and selected bond lengths and angles are listed in Tables 2 and 3; the cation of **3b** has a crystallographically imposed twofold axis of symmetry. Whereas the gross solid-state structural features of **3a** and **3b** are similar, there are marked differences in the coordination parameters of the metal ions. Since the ionic radius of U^{III} is 0.01 Å larger than that of Ce^{III},[20] it is noteworthy that the average U–C distance is 0.04 Å shorter than the average Ce–C distance and, more significantly, the average U–N distance is 0.18 Å shorter than the average Ce–N distance. Concomitantly, the N2-U-N2′ angle of 131.59(18)° is larger than the N2-Ce-N3 angle of 125.1(3)°. The difference of about 0.2 Å between the Ce–N and U–N distances in **3a** and **3b** is the greatest so far observed in analogous cerium(III) and uranium(III) complexes with aromatic nitrogen bases,[4–6] together with that of 0.1 Å found in [M-(Cp*)$_2$I(bipy)] complexes [M = Ce (**1a**), U (**1b**)] and the Rbtp compounds [M(Rbtp)$_3$]$^{3+}$ [M = Ce, U; Rbtp = 2,6-bis(5,6-dialkyl-1,2,4-triazin-3-yl)pyridine].[5] The U–N distances in **3b** are in fact intermediate between amido U^{IV}–NR$_2$ bond lengths, which are typically 2.15–2.30 Å,[23–25] and U–N(terpy) bond lengths, which average 2.62 and 2.58 Å in uranium(III)[4–6] and uranium(IV) compounds,[6] respectively. The shortening of the U–N distances in **3b** strongly suggests

Table 2. M−N and <M−C> distances [Å] in the complexes.

	M−N1	M−N2	M−N3	⟨M−C⟩
[Ce(Cp*)$_2$(terpy)]I (**3a**)	2.640(8)	2.565(8)	2.586(7)	2.82(2)
[U(Cp*)$_2$(terpy)]I (**3b**)	2.419(5)	2.428(4)		2.78(3)
[U(Cp*)$_2$(terpy)] (**4b**)	2.381(4)	2.434(5)	2.448(4)	2.80(3)
[U(Cp*)$_2$(terpy)][U(Cp*)$_2$I$_2$] (**5b**)	2.441(9)	2.448(9)	2.449(8)	2.77(2) (⟨U1−C⟩)
				2.78(2) (⟨U2−C⟩)
[U(Cp*)$_2${NC$_5$H$_4$(py)$_2$}]I (**6**)	2.313(6)	2.470(7)	2.480(7)	2.763(11)
[U(Cp*)$_2${NC$_5$H$_4$(py)$_2$}][BPh$_4$] (**6'**)	2.351(6)	2.471(7)	2.484(7)	2.75(4)
[U(Cp*)$_2${NC$_5$H$_8$(py)$_2$}]I (**7**)	2.247(7)	2.490(7)	2.515(7)	2.77(4)

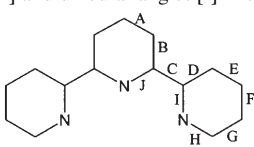partial reduction of the terpy ligand to the radical anion terpy$^{·−}$.

Reduction of **3a** and **3b** with 2% sodium amalgam in THF gave the neutral complexes [M(Cp*)$_2$(terpy)] [M=Ce (**4a**) or U (**4b**); Eq. (4)]. After evaporation of the solvent and extraction into toluene, green powders of **4a** and **4b** were recovered in 92 and 90% yield, respectively; crystals of **4b** were obtained on cooling a diethyl ether solution. Complexes **4a** and **4b** were transformed back into **3a** and **3b** by oxidation with AgI in THF (NMR experiments). Complexes **4**, in which the terpy ligand is reduced to its radical anion form, are trivalent compounds like [Yb(Cp*)$_2$(L)] (L=bipy, phen, terpy), as revealed by magnetic studies (vide infra).

$$[M(Cp^*)_2(terpy)]I + Na(Hg) \rightarrow [M(Cp^*)_2(terpy)] + NaI$$
$$M = Ce \ (\mathbf{4a}) \tag{4}$$
$$M = U \ (\mathbf{4b})$$
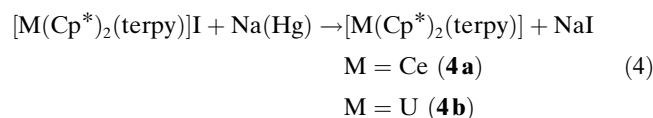
The crystal structure of **4b** is very similar to that of the cation of **3b**, with almost identical average U−C and U−N distances (Table 2). Crystals of the cerium analogue **4a** were not obtained, and the geometrical parameters of **4b** can only be compared with those of the previously reported ytterbium congener.[12] The U−N distances in **4b** are practical-ly equal to the Yb−N distances, although the ionic radius of U^{III} is 0.15 Å larger than that of Yb^{III}.[20] Although the Yb−N distances would be abnormally large due to steric effects,[12] the U−N distances appear signifi-cantly shorter than those pre-dicted from a purely ionic bond-ing model. The greatest devia-tions of the U−N distances in **1b**, **3b**, and **4b** from an electro-static bonding model, by comparison with those noted in the other analogous lanthanide(III) and uranium(III) complexes with polydentate nitrogen ligands,[3–6] can be explained by the greater electron richness and π-donating capacity of the U(Cp*)$_2$ moiety, and electron transfer from the metal to a single instead of several π-acceptor ligands.

Extensive electron transfer in the uranium complexes **3b** and **4b** would lead to filling of the LUMO of neutral terpy and, eventually, to metal oxidation.[17] While the electronic structure of the cationic cerium complex **3a** can be well de-picted by canonical form I in Scheme 1, that is, [Ce^{III}(Cp*)$_2$-(terpy^0)]$^+$, resonance hybrids such as II–IV with the metal centre in the formal oxidation state +4 and a radical anion ligand, that is, [U^{IV}(Cp*)$_2$(terpy$^{·−}$)]$^+$, should make signifi-cant contributions to the true structure of the uranium ana-logue **3b**. That would explain why the U−N bond lengths in **3b** are shorter than the corresponding Ce−N distances in **3a**. Similarly, in the neutral cerium compound **4a**, as in the aforementioned adducts of Ln(Cp*)$_2$ (Ln=Sm, Yb) with π-accepting nitrogen Lewis bases,[8,9,11] the metal centre is in the formal oxidation state +3 and the terpy ligand in its radical anion form, that is, [Ce^{III}(Cp*)$_2$(terpy$^{·−}$)], whereas the structure of the uranium counterpart **4b** could also be described by hybrids resulting from electron transfer from the metal to the ligand, that is, [U^{IV}(Cp*)$_2$(terpy$^{2−}$)]. Only the canonical forms V and VI of the neutral complexes, in
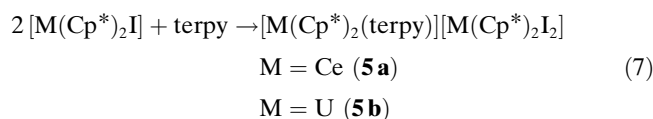
Table 3. Comparison of averaged C−C and C−N bond lengths [Å] and dihedral angles [°] in the terdentate ligands.[a]

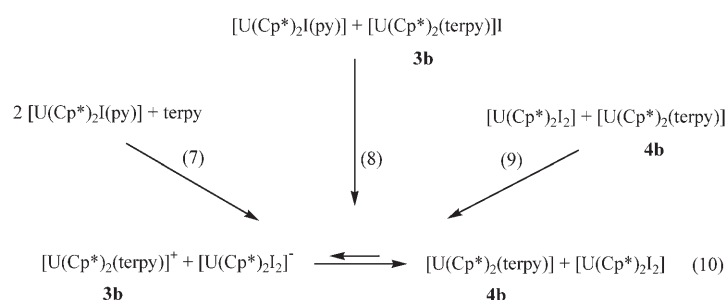| Compound	A	B	C	D	E	F	G	H	I	J	θ[b]
terpy[26]	1.378(3)	1.397(2)	1.490(3)	1.37(3)	1.386(1)	1.36(1)	1.37(2)	1.342(4)	1.33(2)	1.350(3)	
[SnPh$_3$Cl(H$_2$O)]·terpy[27]	1.367(6)	1.393(2)	1.487(8)	1.397(6)	1.374(2)	1.37(1)	1.383(2)	1.338(5)	1.342(5)	1.344(7)	
[UO$_2$(OTf)$_2$(terpy)][28]	1.376(2)	1.398(8)	1.472(1)	1.389(9)	1.38(1)	1.38(1)	1.382(4)	1.347(1)	1.360(4)	1.352(8)	
[Ce(Cp*)$_2$(terpy)]I (**3a**)	1.370(1)	1.384(7)	1.491(13)	1.389(2)	1.385(7)	1.385(15)	1.386(11)	1.326(2)	1.354(8)	1.345(2)	4.5(7); 0.5(7)
[U(Cp*)$_2$(terpy)]I (**3b**)	1.373(6)	1.393(7)	1.449(7)	1.396(7)	1.364(8)	1.391(8)	1.362(7)	1.348(6)	1.372(6)	1.390(5)	0.8(3)
[U(Cp*)$_2$(terpy)][U(Cp*)$_2$I$_2$](**5b**)	1.39(2)	1.366(3)	1.446(6)	1.410(5)	1.366(12)	1.360(6)	1.38(2)	1.358(8)	1.385(4)	1.385(16)	5.5(9); 0.2(9)
[Yb(Cp*)$_2$(terpy)][12]	1.39(2)	1.40(1)	1.46(2)	1.40(1)	1.38(2)	1.38(2)	1.37(1)	1.34(1)	1.40(1)	1.37(1)	6.3; 6.3
[U(Cp*)$_2$(terpy)] (**4b**)	1.393(4)	1.384(2)	1.426(15)	1.411(1)	1.371(1)	1.409(2)	1.367(8)	1.363(6)	1.384(6)	1.416(3)	3.9(2); 6.7(2)
[U(Cp*)$_2${NC$_5$H$_4$(py)$_2$}]I (**6**)	1.47(3)	1.342(11)	1.467(7)	1.409(6)	1.374(4)	1.375(6)	1.379(6)	1.351(12)	1.357(3)	1.426(1)	4.1(7); 3.4(6)
[U(Cp*)$_2${NC$_5$H$_4$(py)$_2$}]BPh$_4$ (**6'**)	1.489(1)	1.350(5)	1.468(15)	1.396(1)	1.374(10)	1.393(1)	1.361(2)	1.361(4)	1.357(9)	1.403(3)	17.8(5); 16.1(5)
[U(Cp*)$_2${NC$_5$H$_8$(py)$_2$}]I (**7**)	1.524(4)	1.483(6)	1.500(7)	1.394(2)	1.377(6)	1.368(15)	1.372(11)	1.361(3)	1.334(7)	1.467(8)	30.2(4); 24.4(5)

[a] Standard deviations of averaged values are given in parentheses. [b] Dihedral angles between the central and lateral rings of the terdentate ligand.

Scheme 1. Canonical forms of complexes **3**; I for M=Ce, I–IV for M=U.

Scheme 2. Canonical forms of complexes **4**; V for M=Ce, V and VI for M=U.

which the radical or the negative charge on the ligand are located at the 4′-position, are represented in Scheme 2.

Successive filling of the LUMO of neutral terpy can be tentatively perceived through the small but systematic variations in the interatomic distances of the terdentate ligand, in a manner similar to that applied to the bipy ligand.[10,21,22] In Table 3, the C−C and C−N bond lengths in **3a**, **3b** and **4b** are listed. These distances can be compared with those of free *anti,anti*-terpy[0],[26] hydrogen-bonded *syn,syn*-terpy[0] in [SnPh₃Cl(H₂O)]·terpy,[27] η³-coordinated terpy[0] in [UO₂-(OSO₂CF₃)₂(terpy)][28] and terpy·− in [Yb(Cp*)₂(terpy)].[12] While a number of d transition metal complexes with terpy²⁻ ligands have been synthesized and studied by electrochemistry, to the best of our knowledge,[29] none of these has been characterized by X-ray diffraction analysis. On the basis of the lengths of bonds A–J, the terpy ligand in the cationic cerium complex **3a** appears to be neutral, in agreement with resonance form I. However, in the uranium analogue **3b**, the C−N bonds H, I, and J are longer, by 0.02–0.04 Å, and the C−C bond C is shorter, by 0.04 Å, than the corresponding bonds in **3a**. It is noteworthy that the differences between the bond lengths of the terpy ligands of **3a** and **3b** are close to those found between **3a** and [Yb(Cp*)₂(terpy)]. These deviations could reflect the contribution, in the true structure of **3b**, of hybrids like II–IV with terpy·− ligands. As expected for the further filling of the LUMO of terpy, the C−C bond C in **4b** is shorter than in **3b**, by about 0.02 Å, while the C−N bonds H, I and J seem to be longer, by 0.01–0.03 Å. The deviations of the bond lengths in the terpy ligand of **4b** from the corresponding ones in [Yb(Cp*)₂(terpy)], in particular the short-

ening of bond C and lengthening of bonds H and J, suggest that hybrids with a terpy²⁻ ligand would contribute to the true structure of **4b**.

The ¹H NMR signals corresponding to the terpy ligands are much more shifted for complexes **4** than for **3**, in agreement with the transformation of terpy[0] into terpy·−; thus, the chemical shifts of the protons of **3a** range from $\delta = 5.98$ to -16.28, whereas those of **4a** range from $\delta = 6.04$ to -310.6.

Electron-transfer reactions of the [M(Cp*)₂(terpy)]ⁿ⁺ complexes (M=Ce, U; n=1, 0); synthesis and crystal structure of [U(Cp*)₂(terpy)][U(Cp*)₂I₂]: The ¹H NMR spectra of mixtures of **3a** and **4a**, or **3b** and **4b**, in pyridine exhibit single averaged resonances corresponding to the Cp* and terpy ligands of each individual compound, that is, rapid and reversible electron-transfer reactions occur [Eq. (5)].

$$[M(Cp^*)_2(\text{terpy})]^+ \underset{-e}{\overset{+e}{\rightleftharpoons}} [M(Cp^*)_2(\text{terpy})]$$
$$\mathbf{3} \qquad\qquad\qquad \mathbf{4} \qquad (5)$$

Similar electron transfer was found to occur in pyridine between the cerium and uranium complexes. Starting from **3a** and **4b**, or **3b** and **4a**, in a 1:1 molar ratio gave the same equilibrating mixture [Eq. (6)]; the NMR spectra again show single averaged resonances for the Cp* and terpy ligands of the cerium and uranium species, and their chemical shifts, by comparison with those of each individual [M-(Cp*)₂(terpy)]I and [M(Cp*)₂(terpy)] complex, indicate that **3a** and **4b** are preponderant, with relative proportions [**3a**]/[**4a**] = [**4b**]/[**3b**] = 87/13.

$$[\text{Ce}(Cp^*)_2(\text{terpy})]^+ + [\text{U}(Cp^*)_2(\text{terpy})] \rightleftharpoons [\text{Ce}(Cp^*)_2(\text{terpy})] + [\text{U}(Cp^*)_2(\text{terpy})]^+$$
$$\mathbf{3a} \qquad\qquad \mathbf{4b} \qquad\qquad \mathbf{4a} \qquad\qquad \mathbf{3b} \qquad (6)$$

While uranium(III) compounds are generally more efficient reducing reagents than their cerium counterparts, these results clearly demonstrate that **3b** is more easily reduced than **3a**; this difference is in agreement with the occurrence of electron transfer in the actinide complex and the contribution of canonical forms with the metal in the formal +4 oxidation state.

Similarly to the synthesis of [Yb(Cp*)₂(bipy)]-[Yb(Cp*)₂Cl₂] from a 2:1 mixture of [Yb(Cp*)₂Cl(thf)] and bipy,[10] the reaction of [Ce(Cp*)₂I] or [U(Cp*)₂I(py)] with

0.5 mol equivalent of terpy in THF led to formation of the complexes $[M(Cp^*)_2(terpy)][M(Cp^*)_2I_2]$ [M=Ce (**5a**), M=U (**5b**); Eq. (7)]. The uranium complex **5b** was isolated as a dark green powder in 93% yield; the cerium analogue **5a** was characterized only by its ^{1}H NMR spectrum.

$$2\,[M(Cp^*)_2I] + terpy \rightarrow [M(Cp^*)_2(terpy)][M(Cp^*)_2I_2]$$
$$M = Ce\ (\mathbf{5a}) \qquad\qquad (7)$$
$$M = U\ (\mathbf{5b})$$

The ^{1}H NMR spectrum of uranium complex **5b** in THF, which exhibits two distinct signals corresponding to the Cp* ligands, is identical to that obtained by mixing **4b** and [U-(Cp*)$_2$I$_2$] or **3b** and [U(Cp*)$_2$I(py)] in the molar ratio of 1:1, as depicted by Equations (8) and (9) in Scheme 3; the chem-

$[U(Cp^*)_2I(py)] + [U(Cp^*)_2(terpy)]I$

3b

$2\,[U(Cp^*)_2I(py)] + terpy$ $[U(Cp^*)_2I_2] + [U(Cp^*)_2(terpy)]$

(7)   (8)   (9)   **4b**

$[U(Cp^*)_2(terpy)]^+ + [U(Cp^*)_2I_2]^- \longleftarrow\longrightarrow [U(Cp^*)_2(terpy)] + [U(Cp^*)_2I_2]$ (10)

3b   **4b**

Scheme 3. Electron-transfer reactions between **3b**, **4b**, [U(Cp*)$_2$I$_2$] and [U(Cp*)$_2$I$_2$]$^-$.

ical shifts of the Cp* and terpy signals are between those of **3b** and **4b** and those of [U(Cp*)$_2$I$_2$]$^-$ and [U(Cp*)$_2$I$_2$]. The latter iodo complexes of uranium(III) and uranium(IV) were readily obtained by treating [U(Cp*)$_2$I(py)] with NEt$_4$I and AgI, respectively. These results revealed that the electron-transfer reaction depicted by Equation (10) in Scheme 3 occurs in THF solution; from the chemical shifts of the averaged Cp* resonances, the relative proportions of **3b** and **4b**, and of [U(Cp*)$_2$I$_2$]$^-$ and [U(Cp*)$_2$I$_2$], are about 35:65. Formation of complexes **5** was not observed in pyridine, and the NMR spectrum of **5b** in this solvent exhibits the signals corresponding to the individual complexes **3b** and [U-(Cp*)$_2$I(py)].

Crystals of **5b**·toluene suitable for X-ray diffraction analysis were obtained by slow diffusion of pentane into a toluene solution; a view of **5b** is shown in Figure 3. The 1:1 stoichiometry of the two components of **5b** suggests the presence of cation–anion pairs. The U1–N distances, as well as the C–C and C–N distances within the terpy ligand are expectedly very similar to those found in **3b** and **4b** (Tables 2 and 3). However, the three U1–N distances are quite identical, as found in **3b**. The U2–I1 and U2–I2 distances, with a mean value of 3.1038(14) Å, are at the lower limit of the range of uranium(III)–iodide distances, which range from 3.103(2) Å in [UI$_3$(thf)$_4$][30] to 3.273(1) Å in [UI$_2$-(terpy)$_2$(py)]I·2py.[4] However, these distances are larger

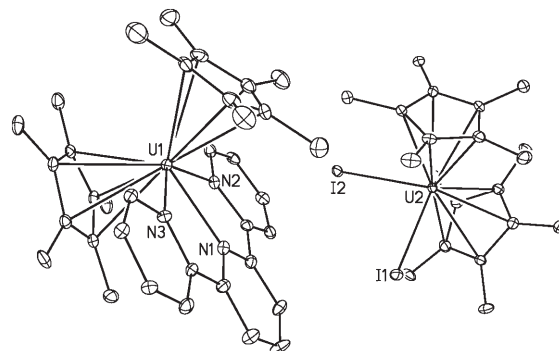than the uranium(IV)–iodide distances, which are typically 3.0 Å.[31]

Figure 3. Crystal structure of [U(Cp*)$_2$(terpy)][U(Cp*)$_2$I$_2$] (**5b**) with thermal ellipsoids drawn at the 10% probability level. H atoms have been omitted.

Magnetic properties of $[M(Cp^*)_2(terpy)]^{n+}$ (M=Ce, U; $n=$ 1, 0): The magnetic behavior of **3a** and **4a** is shown in Figure 4. For **3a**, in which the terpy ligand is diamagnetic,
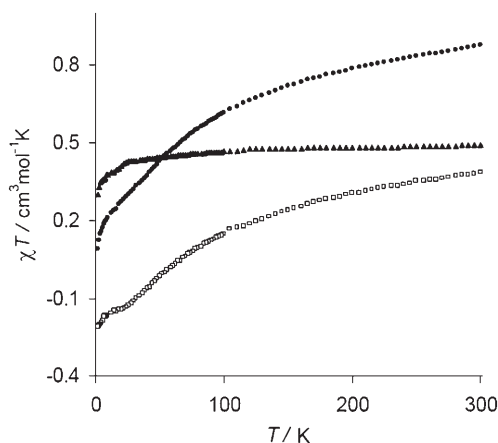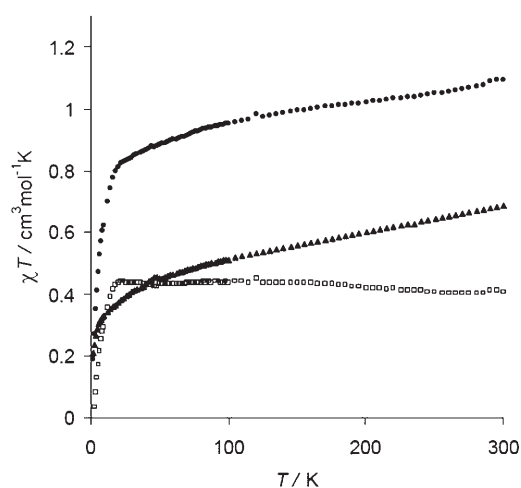

Figure 4. Thermal dependence of $\chi_{3a}T$ (▲), $\chi_{4a}T$ (●) and the difference $\Delta\chi T = \chi_{4a}T - \chi_{3a}T$ (□).

the $\chi_{3a}T$ value represents the contribution of the sole Ce^{3+} ion in its crystal field;[32] it decreases with decreasing T, due to depopulation of the Stark sublevels, and reaches 0.3 cm^{3}Kmol^{-1} at 2 K. The temperature dependence of $\chi_{4a}T$ for **4a** is the result of the superimposition of both the variation of the intrinsic susceptibility of the Ce^{3+} ion and the Ce^{III}–terpy$^{•-}$ interaction; at 300 K, the value of 0.8 cm^{3}Kmol^{-1} is close to that expected for the two uncorrelated spin carriers. Since the structures of **4a** and the cation of **3a** are likely to be quite identical, and therefore crystal fields around the Ce atoms are very similar in the two complexes, it is possible to apply the empirical method devised by Kahn et al.[33] and Costes et al.[34] to determine the nature of the exchange interaction. The sign, but not the value of the coupling constant, of the Ce^{III}–terpy$^{•-}$ interaction in **4a**

can be obtained by subtracting from $\chi_{4a}T$ the contribution arising from thermal depopulation of the Stark sublevels of Ce^{III}, that is, $\chi_{3a}T$. In the absence of a general theoretical model to describe the magnetic susceptibility of a metal ion with a first-order orbital momentum, this strategy of diamagnetic substitution permits the problem of the spin–orbit coupling of this ion to be overcome. The profile of the curve of the difference $\Delta\chi T = \chi_{4a}T - \chi_{3a}T$ versus T (Figure 4) clearly shows that the ground state of **4a** is antiferromagnetically coupled. It is noteworthy that the Ce–spin carrier interaction has been found to be antiferromagnetic for all compounds investigated so far, irrespective of the structural details.[32–35] Comparison of the magnetic properties of [Yb-(Cp*)$_2$(L)]I and [Yb(Cp*)$_2$(L)] (L = bipy or phen) also revealed antiferromagnetic coupling between the Yb^{3+} ion and the ligand radical in the neutral complexes.[10]

The magnetic behavior of **3b** is characteristic of an uranium(III) complex, as shown by the $\chi_{3b}T$ versus T plot in Figure 5, which is similar to that previously reported for a

Figure 5. Thermal dependence of $\chi_{3b}T$ (▲), $\chi_{4b}T$ (●) and the difference $\Delta\chi T = \chi_{4b}T - \chi_{3b}T$ (□).

variety of trivalent organometallic and inorganic uranium complexes;[36] $\chi_{3b}T$ decreases from 0.7 cm^{3}K mol^{-1} at 300 K to 0.2 cm^{3}K mol^{-1} at 2 K. For **4b**, as for its cerium counterpart **4a**, the value of $\chi_{4b}T = 1.1$ cm^{3}K mol^{-1} at 300 K corresponds to that expected for two noninteracting spin carriers; $\chi_{4b}T$ decreases as T is lowered and reaches 0.2 cm^{3}K mol^{-1} at 2 K. The difference $\Delta\chi T = \chi_{4b}T - \chi_{3b}T$, which decreases with decreasing temperature, reveals that the U^{III}–terpy$^{·-}$ interaction is antiferromagnetic. To the best of our knowledge, the magnetic exchange in **4b** is the first interaction between uranium(III) and a spin carrier to have been characterized in a molecular compound.

Reactions of [M(Cp*)$_2$(terpy)]$^{n+}$ (M = Ce, U; n = 1, 0) with Ph$_3$SnH and NEt$_3$HBPh$_4$; synthesis and characterization of [U(Cp*)$_2${NC$_5$H$_n$(py)$_2$}]X (n = 4, 8; X = I, BPh$_4$): The reactions of **3** and **4** with the H$^·$ and H$^+$ donor reagents Ph$_3$SnH

and NEt$_3$HBPh$_4$ led to a clear differentiation of the cerium and uranium complexes. No reaction was observed between these reagents and **3a**, as expected for a neutral terpy ligand coordinated to Ce^{III} (resonance form I in Scheme 1). In contrast, treatment of the uranium counterpart **3b** with Ph$_3$SnH in pyridine readily afforded the uranium(IV) compound [U-(Cp*)$_2${NC$_5$H$_4$(py)$_2$}]I (**6**), where NC$_5$H$_4$(py)$_2$ is the 2,6-dipyridyl(hydro-4-pyridyl) ligand (Scheme 4). Dark brown crys-
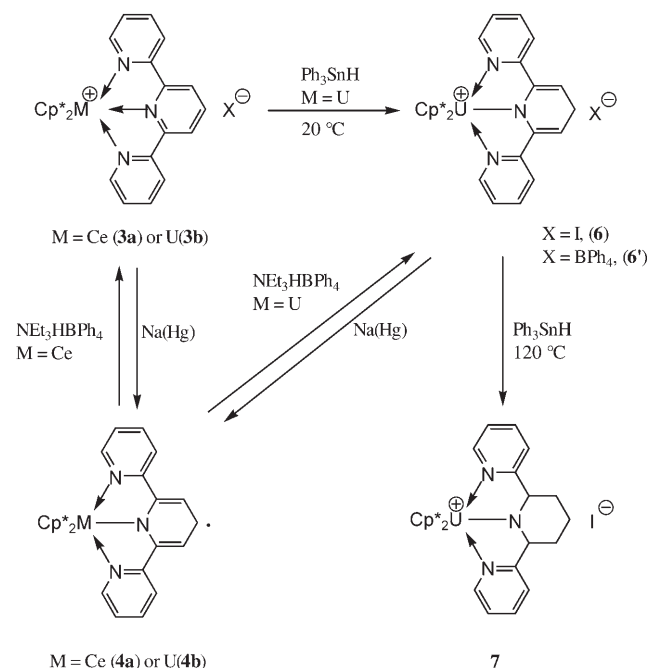
Scheme 4. Distinct reactions of the cerium and uranium complexes.

tals of **6**·py suitable for X-ray diffraction analysis were obtained by slow diffusion of pentane into a pyridine solution. To the best of our knowledge, **6** is the first complex with a monohydroterpyridyl ligand. However, nucleophilic attack on both the 2- and 4-positions of pyridine is well documented.[37] Various yttrium complexes of the type [Y]-(η^1-NC$_5$H$_6$) were synthesized by reaction of pyridine and yttrium hydrides;[38] in the case of [Y(C$_5$H$_5$)$_2$(NC$_5$H$_6$)],[38a] it was demonstrated that the 1,4-addition product was obtained after slow isomerization of the initially formed 1,2-addition product. No indication for a 1,2-addition product was found in the reaction of **3b** and Ph$_3$SnH, and the formation of **6** can obviously be accounted for by the direct addition of H$^·$ onto the 4′-position of the terpy ligand in canonical form II (Scheme 1), which confirms the contribution of this hybrid to the true structure of **3b**.

Complex **6** was further hydrogenated to [U(Cp*)$_2$-{NC$_5$H$_8$(py)$_2$}]I (**7**) by using an excess of Ph$_3$SnH in refluxing pyridine (Scheme 4); after evaporation of the solvent and washing with THF, the orange powder of **7** was isolated in 68 % yield, and crystals suitable for X-ray diffraction analysis were deposited from a THF solution.

Treatment of the cerium complex **4a** with NEt_3HBPh_4 led to oxidation of the terpy$^{·-}$ ligand and formation of [Ce-$(Cp^*)_2(terpy)]BPh_4$. Similar reaction with **4b** followed a distinct course and afforded the uranium(IV) complex [U-$(Cp^*)_2\{NC_5H_4(py)_2\}]BPh_4$ (**6′**), which was isolated as a dark brown powder in 81 % yield; crystals of **6′** were obtained by crystallization from THF. The synthesis of **6′**, which clearly results from the addition of H^+ to the terpy ligand, strongly supports the contribution of hybrid VI (Scheme 2) to the true structure of **4b**.

Reduction of **6** and **6′** with sodium amalgam in THF gave **4b**; this reaction may involve the neutral uranium(III) intermediate $[U(Cp^*)_2\{NC_5H_4(py)_2\}]$, which would be unstable towards aromatization of the terdentate ligand and loss of dihydrogen.

Compounds **4** appeared to be inert in the presence of Ph_3SnH. It is possible that the expected cerium product [Ce-$(Cp^*)_2\{NC_5H_4(py)_2\}]$, like its uranium analogue, is unstable towards aromatization of the terdentate ligand, giving back **4a** in a degenerate process; however, dihydrogen was not detected in the reaction mixture.

Complex **5b** reacted in THF with either Ph_3SnH or NEt_3HBPh_4 to give the cation $[U(Cp^*)_2\{NC_5H_4(py)_2\}]^+$, a result which is in agreement with the fact that **5b** is actually an equilibrating mixture of **3b** and **4b** in THF solution ([Eq. (10)] in Scheme 3).

Complexes **6**, **6′** and **7** are composed of discrete cation–anion pairs; a view of the cation of **6**, which is very similar to that of **6′**, and a view of the cation of **7** are shown in Figures 6 and 7, respectively, while selected bond lengths and
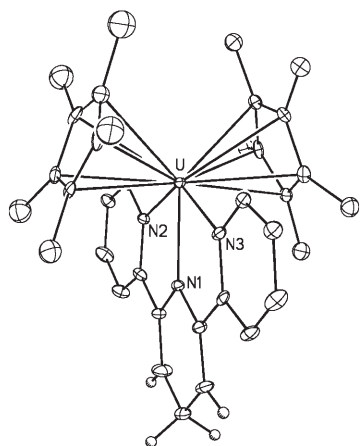

Figure 7. Crystal structure of the cation in $[U(Cp^*)_2\{NC_5H_8(py)_2\}]I$ (**7**) with thermal ellipsoids drawn at the 10 % probability level. H atoms have been omitted.

tween the uranium atom and the central nitrogen atom of the monohydroterpyridyl ligand of 2.313(6) and 2.351(6) Å in **6** and **6′**, respectively, are shorter, by 0.03–0.13 Å, than those in the other uranium complexes, while the U−N2 and U−N3 distances are longer, by 0.03–0.04 Å. The lengths of the C−C bonds A and B and C−N bond J in the terdentate ligands of **6** and **6′** clearly correspond to the respective single, double and single character of these bonds. The U−N1 distance is even shorter in **7**, with a value of 2.247(7) Å, which is typical of an amide ligand terminally coordinated to uranium(IV),[23–25] while the U−N2 and U−N3 distances are even larger (2.490(7) and 2.515(7) Å, respectively). The lengthening of the U−N1 distances in **6** and **6′** with respect to **7** could reflect some charge delocalization and the contribution to the true structure of resonance forms such as VII in Scheme 5. In agreement with this assumption, C−N bond

Figure 6. Crystal structure of the cation in $[U(Cp^*)_2\{NC_5H_4(py)_2\}]I$ (**6**) with thermal ellipsoids drawn at the 10 % probability level. H atoms have been omitted except those at the 3-, 4- and 5-positions of the central ring.

Scheme 5. Canonical forms of complexes **6**.

J in **7** appears to be longer than in **6** and **6′**, by about 0.05 Å, while B is clearly a single C−C bond. The C−C bonds C in **6**, **6′** and **7** are 0.02–0.05 Å longer than in the other uranium complexes **3b**, **4b** and **5b**. In **7**, bond C is identical to that in free terpy, and the terdentate ligand is not planar, with dihedral angles between the mean planes of the central and lateral rings of 30.2(4) and 24.4(5)°. The central ring of the $NC_5H_8(py)_2$ ligand in **7** adopts a chair conformation which brings the C2, C3 and C4 atoms out of the mean plane defined by the other atoms of the terdentate ligand (rms devi-

angles are listed in Tables 2 and 3. The structures are of good quality and the sp^3 nature of C3 in **6** and **6′**, and of C2, C3, and C4 in **7** is clear-cut. While the uranium environment in these cations is similar to that in **3–5**, significant structural differences are easily discernible. The U−N1 distances be-
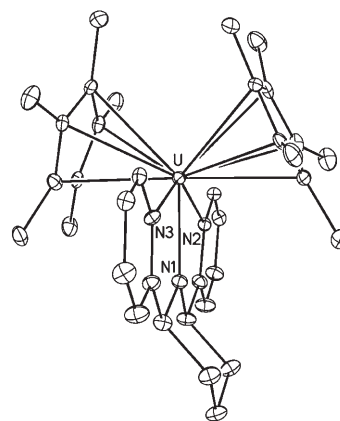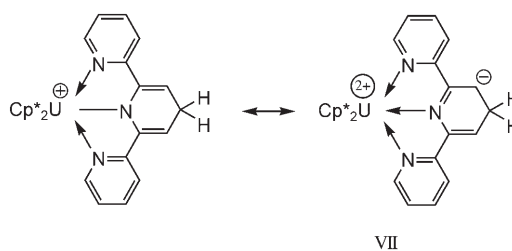
ation 0.058 Å), which lies in the equatorial girdle of the U-(Cp*)$_2$ moiety; the dihedral angle between this plane and the C2-C3-C4 plane is 3.1(8)°. The solid-state structure of **7** is preserved in solution, as shown by the ^{1}H NMR spectrum, which exhibits two distinct signals of equal intensity (15 H) corresponding to the Cp* ligands, and two distinct signals of equal intensities (1 H) attributed to the protons on C3 carbon.

The magnetic behavior of **6′** (Figure 8) is characteristic of a tetravalent uranium compound;[39] $\chi_{6'}T$ decreases from 0.8 cm^{3}K mol^{-1} at 300 K to 0 cm^{3}K mol^{-1} at 2 K, since the local ground state of the uranium(IV) site is nonmagnetic.
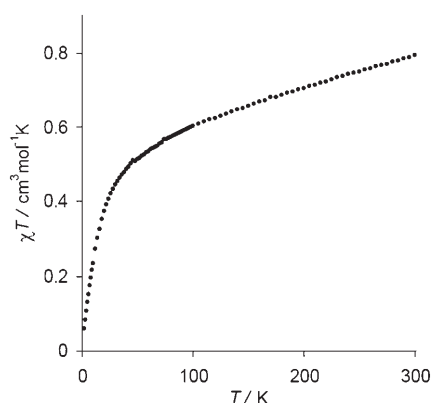
Figure 8. Thermal dependence of $\chi_{6'}T$.

Conclusion

Comparison of the crystal structures of [M(Cp*)$_2$I(bipy)] [M = Ce (**1a**), M = U (**1b**)] indicated that the extent of donation of electron density into the LUMO of the bidentate ligand is more important in the actinide than in the lanthanide compound. The synthesis of the terpyridine complexes [M(Cp*)$_2$(terpy)] [M = Ce (**4a**), M = U (**4b**)] by reduction of the cationic precursors [M(Cp*)$_2$(terpy)]I [M = Ce (**3a**), M = U (**3b**)] permitted for the first time the structural and physicochemical properties of such low-valent compounds of 4f and 5f elements to be compared. Rapid electron-transfer reactions between complexes **3** and **4** in solution were revealed by NMR spectroscopy. Magnetic studies indicated that the uranium atoms in **3b** and **4b** are in the +3 oxidation state. Compound **4b**, like its cerium counterpart, should be formulated as [M^{III}(Cp*)$_2$(terpy$^{·-}$)], in which spins on the individual units are antiferromagnetically coupled at low temperature; the exchange interaction in **4b** is the first uranium(III)–spin carrier interaction to have been characterized in a molecular complex. However, comparison of the crystal structures and reactions of these analogous cerium-(III) and uranium(III) complexes revealed significant differences which reflect the presence of stronger electron transfer between the electron-rich metal and the terdentate N ligand

in the actinide compounds. The shortening of the U−N distances with respect to the Ce−N distances is the most pronounced so far observed in such pairs of trivalent lanthanide and actinide complexes; the small but systematic variations in the C−C and C−N bond lengths of the terdentate ligands also indicate more extensive filling of the LUMO of terpy in the uranium than in the cerium compounds. The contribution of the canonical forms [U^{IV}(Cp*)$_2$(terpy$^{·-}$)]I and [U^{IV}-(Cp*)$_2$(terpy^{2-})] to the true structures of **3b** and **4b** was strongly evidenced by the reactions of these complexes with Ph$_3$SnH and NEt$_3$HBPh$_4$, respectively, which afforded the cation [U(Cp*)$_2${NC$_5$H$_4$(py)$_2$}]$^+$, the first metal complex with a monohydroterpyridyl ligand. These results, together with those concerning the selective complexation of uranium(III) over lanthanide(III) ions by aromatic nitrogen bases,[4,5,16,17] clearly demonstrate that the presence of electron transfer in the 5f element complexes is of the greatest importance for favoring clear-cut Ln^{III}/An^{III} differentiation.

Experimental Section

The ^{1}H NMR spectra were recorded on a Bruker DPX 200 instrument and referenced internally by using the residual proton solvent resonances relative to tetramethylsilane ($\delta = 0$). Magnetic susceptibility data were collected on a powdered sample of the compound with a SQUID-based sample magnetometer Quantum design MPMS5. Elemental analyses were performed by Analytische Laboratorien at Lindlar (Germany).

CeI$_3$, terpy, NEt$_4$I, AgI (Aldrich), and Ph$_3$SnH (Janssen) were used without purification. NEt$_3$HBPh$_4$ was prepared by mixing NEt$_3$HCl and NaBPh$_4$ in water; the precipitate was filtered off, washed with ethanol and diethyl ether and dried under vacuum. The green powder of [U-(Cp*)$_2$I(py)] was obtained by evaporation of a pyridine solution of [U-(Cp*)$_2$I(thf)], which was prepared as previously reported;[40] in contrast to the cerium analogue, the pyridine ligand in [U(Cp*)$_2$I(py)] is not labile and did not dissociate on heating under vacuum. ^{1}H NMR ([D$_6$]benzene, 23°C): $\delta = 5.02$ (s, 1 H; py), −1.64 (s, 30 H; Cp*), −10.50 (s, 2 H; py), −70.50 ppm (s, 2 H; py).

Synthesis of [Ce(Cp*)$_2$I]: A flask was charged with CeI$_3$ (1070 mg, 2.05 mmol) and KCp* (718 mg, 4.12 mmol), and THF (20 mL) was condensed into it. The yellow reaction mixture was stirred at 20°C for 24 h. The solvent was evaporated, and the pink residue extracted with a mixture of THF (0.5 mL) and toluene (20 mL). The solution was evaporated to dryness, leaving the product as a bright pink powder (970 mg, 88%). ^{1}H NMR ([D$_8$]THF, 23°C): $\delta = 5.35$ ppm (Cp*); elemental analysis calcd (%) for C$_{20}$H$_{30}$ICe (537): C 44.69, H 5.63; found: C 44.47, H 5.53.

Synthesis of [Ce(Cp*)$_2$I(bipy)] (1a): A flask was charged with [Ce-(Cp*)$_2$I] (20 mg, 0.036 mmol) and bipy (6.0 mg, 0.038 mmol) in THF (0.4 mL). After 1 h at 20°C, the solvent was evaporated, leaving an orange powder of **1a**, which was washed with Et$_2$O (0.3 mL) and dried under vacuum (20.2 mg, 81%). ^{1}H NMR ([D$_8$]THF, 23°C): $\delta = 10.75$ (s, 30 H; Cp*), 8.94 (s, 1 H; bipy), 7.10 (s, 1 H; bipy), 6.59 (s, 1 H; bipy), 6.05 (s, 1 H; bipy), 4.27 (s, 1 H; bipy), 0.90 (s, 1 H; bipy), −32.5 ppm (s, 2 H; bipy); elemental analysis calcd (%) for C$_{30}$H$_{38}$IN$_2$Ce (693.7): C 51.95, H 5.52, N 4.04; found: C 52.04, H 5.37, N 4.22.

Synthesis of [U(Cp*)$_2$I(bipy)] (1b): By using the same procedure as for **1a**, reaction of [U(Cp*)$_2$I(py)] (204 mg, 0.286 mmol) and bipy (47 mg, 0.30 mmol) in THF (10 mL) gave a black powder of **1b** (163 mg, 72%).

^{1}H NMR ([D$_8$]THF, 23°C): $\delta = 4.56$ (s, 30 H; Cp*), 27.52 (s, 1 H; bipy), 15.07 (s, 1 H; bipy), −0.19 (s, 1 H; bipy), −0.46 (s, 1 H; bipy), −2.05 (s, 1 H; bipy), −4.78 (s, 1 H; bipy), −37.91 (s, 1 H; bipy), −40.92 ppm (s, 1 H; bipy); elemental analysis calcd (%) for C$_{30}$H$_{38}$IN$_2$U (791.6): C 45.52, H 4.84, N 3.54, I 16.03; found: C 45.35, H 4.74, N 3.68, I 15.96.

Reaction of [Ce(Cp*)$_2$I] with bipy: An NMR tube was charged with **1a** (7.2 mg, 0.013 mmol) and 2% Na(Hg) (17.2 mg, 0.015 mmol of Na) in [D$_8$]THF (0.4 mL). The mixture was heated for 12 h in a sand bath at 110°C, and the spectrum of the brown solution showed that **2a** was formed in almost quantitative yield. ^{1}H NMR ([D$_8$]THF, 23°C): $\delta = 4.17$ (s, 30 H; Cp*), −26.91 (s, 2 H; bipy), −40.46 (s, 2 H; bipy), −159.23 (s, 2 H; bipy), −253.11 ppm (s, 2 H; bipy).

Synthesis of [U(Cp*)$_2$(bipy)] (2b): A flask was charged with **1b** (150 mg, 0.189 mmol) and 2% Na(Hg) (280 mg, 0.243 mmol of Na), and THF (10 mL) was condensed into it. The mixture was stirred at 20°C for 12 h, the solvent was evaporated, and the residue extracted with toluene (15 mL). The solution was evaporated to dryness and the green powder of **2b** was dried under vacuum (75.5 mg, 80%). ^{1}H NMR ([D$_8$]toluene, 23°C): $\delta = 0.25$ (s, 30 H; Cp*), −19.8 (d, $J = 6$ Hz, 2 H; bipy), −41.58 (t, $J = 6$ Hz, 2 H; bipy), −81.40 (t, $J = 6$ Hz, 2 H; bipy), −93.91 ppm (t, $J = 6$ Hz, 2 H; bipy); elemental analysis calcd (%) for C$_{30}$H$_{38}$N$_2$U (664.7): C 54.21, H 5.76, N 4.21; found: C 54.16, H 5.84, N 4.31.

^{1}H NMR characterization of [U(Cp*)$_2$I$_2$] and [NEt$_4$][U(Cp*)$_2$I$_2$]: a) An NMR tube was charged with [U(Cp*)$_2$I(py)] (10.1 mg, 0.014 mmol) and AgI (3.3 mg, 0.014 mmol) in [D$_8$]THF (0.4 mL). The reaction mixture was stirred at 60°C for 12 h; the color of the solution turned from green to orange, and black metallic silver was deposited. The spectrum showed the presence of [U(Cp*)$_2$I$_2$] as the sole product with signals of free pyridine. ^{1}H NMR ([D$_8$]THF, 23°C): $\delta = 18.43$ (Cp*). b) An NMR tube was charged with [U(Cp*)$_2$I(py)] (12.9 mg, 0.018 mmol) and NEt$_4$I (4.6 mg, 0.018 mmol) in [D$_8$]THF (0.4 mL). The tube was immersed in an ultrasound bath (80 W, 40 kHz) for 1 h. The spectrum of the dark orange solution showed the presence of [NEt$_4$][U(Cp*)$_2$I$_2$] as the sole product. ^{1}H NMR ([D$_8$]THF, 23°C): $\delta = -2.69$ (s, 30 H; Cp*), −6.11 (br, 12 H; CH$_2$*Me*), −6.83 ppm (br, 8 H; C*H*$_2$Me).

Synthesis of [Ce(Cp*)$_2$(terpy)]I (3a): An NMR tube was charged with [Ce(Cp*)$_2$I] (11 mg, 0.02 mmol) and terpy (4.8 mg, 0.02 mmol) in [D$_8$]THF (0.4 mL). The tube was immersed in an ultrasound bath (80 W, 40 kHz) for 15 min. Orange crystals were deposited from the solution at 6°C; these were collected and dried under vacuum (12 mg, 72%). ^{1}H NMR ([D$_5$]py, 23°C): $\delta = 5.98$ (t, $J = 8$ Hz, 1 H; terpy), 5.88 (t, $J = 7$ Hz, 2 H; terpy), 4.33 (s, 30 H; Cp*), 4.16 (d, $J = 9$ Hz, 2 H; terpy), 4.12 (d, $J = 7$ Hz, 2 H; terpy), 2.93 (d, $J = 7$ Hz, 2 H; terpy), −16.28 ppm (s, 2 H; terpy); elemental analysis calcd (%) for C$_{35}$H$_{41}$IN$_3$Ce (770.7): C 54.54, H 5.36, N 5.45; found: C 54.64, H 5.52, N 5.56.

Synthesis of [U(Cp*)$_2$(terpy)]I (3b): A flask was charged with [U-(Cp*)$_2$I(py)] (145 mg, 0.203 mmol) and terpy (52 mg, 0.223 mmol), and THF (12 mL) was condensed into it. The reaction mixture was stirred at 20°C for 4 h and the solvent was evaporated. The black powder of **3b** was washed with THF (10 mL) and dried under vacuum (172 mg, 90%). ^{1}H NMR ([D$_5$]py, 23°C): $\delta = 8.53$ (s, 30 H; Cp*), the terpy signals were very broad and not assigned; ^{1}H NMR ([D$_5$]py, 70°C): $\delta = 13.66$ (s, 2 H; terpy), 7.82 (s, 30 H; Cp*), 4.26 (s, 2 H; terpy), 2.90 (s, 2 H; terpy), −3.16 (s, 2 H; terpy), −57.00 ppm (s, 2 H; terpy); the signal of relative intensity 1 H of the terpy ligand was not detected; elemental analysis calcd (%) for C$_{35}$H$_{41}$IN$_3$U (868.7): C 48.39, H 4.76, N 4.84; found: C 48.25, H 4.81, N 4.97.

Synthesis of [Ce(Cp*)$_2$(terpy)] (4a): A flask was charged with **3a** (100 mg, 0.130 mmol) and 2% Na(Hg) (540 mg, 0.47 mmol), and THF (12 mL) was condensed into it. The reaction mixture was stirred at 20°C for 12 h. The green solution was evaporated to dryness and the residue extracted with toluene (15 mL). After evaporation of the solvent, **4a** was recovered as a green powder (86 mg, 92%). ^{1}H NMR ([D$_8$]THF, 23°C): $\delta = 6.04$ (s, 2 H; terpy), 3.94 (s, 30 H; Cp*), −10.86 (s, 2 H; terpy), −13.97 (s, 2 H; terpy), −68.93 (s, 2 H; terpy), −115.42 (s, 2 H; terpy), −310.6 ppm (s, 1 H; terpy); elemental analysis calcd (%) for C$_{35}$H$_{41}$N$_3$Ce (643.8): C 65.29, H 6.42, N 6.53; found: C 65.15, H 6.59, N 6.70.

Synthesis of [U(Cp*)$_2$(terpy)] (4b): A flask was charged with **3b** (150 mg, 0.173 mmol) and 2% Na(Hg) (800 mg, 0.70 mmol), and THF (12 mL) was condensed into it. The reaction mixture was stirred at 20°C for 12 h. The green solution was evaporated to dryness, and the residue extracted with toluene (15 mL). After evaporation of the solvent, **4b** was recovered as a dark green powder (116 mg, 90%). ^{1}H NMR ([D$_8$]THF, 23°C): $\delta = 15.35$ (s, 30 H; Cp*), −8.35 (s, 2 H; terpy), −20.70 (s, 2 H; terpy), −28.79 (d, $J = 8$ Hz, 2 H; terpy), −41.26 (s, 2 H; terpy), −48.43 (s, 1 H; terpy), −126.40 ppm (s, 2 H; terpy); elemental analysis calcd (%) for C$_{35}$H$_{41}$N$_3$U (741.8): C 56.67, H 5.57, N 5.66; found: C 56.48, H 5.47, N 5.52.

Reactions of complexes 4 with AgI: a) An NMR tube was charged with **4a** (12.2 mg, 0.019 mmol) and AgI (4.4 mg, 0.019 mmol) in THF (0.4 mL). After 30 min in the ultrasound bath, the solution was colorless and orange crystals had deposited; THF was replaced with [D$_5$]py, and the spectrum showed the formation of **3a** as the sole product. b) By using the same procedure, reaction of **4b** (10.9 mg, 0.014 mmol) and AgI (3.4 mg, 0.014 mmol) in THF gave a black powder, and the NMR spectrum in [D$_5$]py showed the formation of **3b**.

Electron transfer reactions between 3a and 4a, or 3b and 4b: a) An NMR tube was charged with **3a** (11.8 mg, 0.015 mmol) and **4a** (9.6 mg, 0.015 mmol) in [D$_8$]THF (0.4 mL). The tube was immersed in the ultrasound bath for 5 min. The spectrum showed the single averaged resonances corresponding to the Cp* and terpy ligands of **3a** and **4a**. ^{1}H NMR ([D$_8$]THF, 23°C): $\delta = 4.27$ (s, 30 H; Cp*), 1.77 (d, $J = 10$ Hz, 2 H; terpy), −4.35 (s, 2 H; terpy), −13.49 (s, 2 H; terpy), −28.67 (s, 2 H; terpy), −52.28 (s, 2 H; terpy), −138.9 ppm (s, 1 H; terpy). b) Similarly, the spectrum of a mixture of **3b** (12.0 mg, 0.014 mmol) and **4b** (10.2 mg, 0.014 mmol) in [D$_8$]THF (0.4 mL) exhibited the single averaged resonances corresponding to the Cp* and terpy ligands of **3b** and **4b**. ^{1}H NMR ([D$_8$]THF, 23°C): $\delta = 12.10$ (s, 30 H; Cp*), 2.40 (s, 2 H; terpy), −9.77 (s, 2 H; terpy), −11.71 (s, 2 H; terpy), −19.41 (s, 2 H; terpy), −96.56 ppm (s, 2 H; terpy); the signal of relative intensity 1 H of the terpy ligand was not detected.

Electron transfer reactions between 3a and 4b, or 3b and 4a: An NMR tube was charged with **3a** (9.4 mg, 0.012 mmol) and **4b** (9.1 mg, 0.012 mmol), or **3b** (12.0 mg, 0.014 mmol) and **4a** (9.1 mg, 0.014 mmol) in [D$_8$]THF (0.4 mL). The tube was immersed in the ultrasound bath for 1 h. The spectra showed the averaged resonances corresponding to the equilibrating mixtures of **3a**, **4a**, **3b** and **4b** with [**3a**]/[**4a**] = [**4b**]/[**3b**] = 87/13.

Reaction of [Ce(Cp*)$_2$I] with 0.5 mol equivalent of terpy: An NMR tube was charged with [Ce(Cp*)$_2$I] (11.0 mg, 0.02 mmol) and terpy (2.4 mg, 0.01 mol) in [D$_8$]THF (0.4 mL). The tube was immersed in the ultrasound bath for 15 min. The spectrum of the orange solution showed the quantitative formation of [Ce(Cp*)$_2$(terpy)][Ce(Cp*)$_2$I$_2$] (5a). ^{1}H NMR ([D$_8$]THF, 23°C): $\delta = 7.08$ (s, 1 H; terpy), 5.10 (s, 30 H; Cp*), 4.34 (s, 2 H; terpy), 3.95 (s, 30 H; Cp*), 2.24 (s, 2 H; terpy), 1.65 (s, 2 H; terpy), 1.00 (s, 2 H; terpy), −16.54 ppm (s, 2 H; terpy).

Synthesis of [U(Cp*)$_2$(terpy)][U(Cp*)$_2$I$_2$] (5b): A flask was charged with [U(Cp*)$_2$I(py)] (123 mg, 0.172 mmol) and terpy (20.0 mg, 0.086 mmol), and toluene (15 mL) was condensed into it. After 1 h at 20°C, the volume of the solution was reduced to 5 mL and addition of pentane (13 mL) induced precipitation of a dark green powder of **5b**, which was filtered off and dried under vacuum (70 mg, 93%). The ^{1}H NMR spectrum of **5b** in [D$_8$]THF is identical to that of a 1:1 mixture of **3b** and [U-(Cp*)$_2$I(py)], or **4b** and [U(Cp*)$_2$I$_2$]. ^{1}H NMR ([D$_8$]THF, 23°C): $\delta = 12.71$ (s, 30 H; Cp*), 11.20 (s, 30 H; Cp*), 2.76 (t, $J = 9$ Hz, 2 H; terpy), −14.28 (s, 2 H; terpy), −17.99 (s, 2 H; terpy), −26.99 (s, 2 H; terpy), −106.2 ppm (s, 2 H; terpy); the signal of relative intensity 1 H of the terpy ligand was not detected; elemental analysis calcd (%) for C$_{55}$H$_{71}$I$_2$N$_3$U$_2$ (1504): C 43.92, H 4.76, N 2.79; found: C 43.65, H 4.72, N 3.01.

Reaction of 3b with Ph$_3$SnH: An NMR tube was charged with **3b** (6.6 mg, 0.0076 mmol) and Ph$_3$SnH (10.0 mg, 0.028 mmol) in [D$_5$]py (0.4 mL). The tube was immersed in the ultrasound bath for 1 h. The spectrum of the dark brown solution showed almost quantitative formation of [U(Cp*)$_2${NC$_5$H$_4$(py)}$_2$]I (6). ^{1}H NMR ([D$_5$]py, 23°C): $\delta = 59.57$ (s, 2 H; N ligand), 16.23 (s, 30 H; Cp*), 0.02 (t, $J = 10$ Hz, 2 H; N ligand),

−10.99 (d, $J = 10$ Hz, 2 H; N ligand), −19.01 (s, 2 H; N ligand), −19.39 (s, 2 H; N ligand), −113.78 ppm (s, 2 H; N ligand).

Reaction of 4a with NEt₃HBPh₄: An NMR tube was charged with **4a** (9.5 mg, 0.015 mmol) and NEt₃HBPh₄ (6.3 mg, 0.015 mmol) in [D₅]py. The tube was immersed in the ultrasound bath for 2 h; bubbles of gas, presumably dihydrogen, were observed in the early stages of the reaction. The spectrum of the green solution showed almost quantitative formation of [Ce(Cp*)₂(terpy)]BPh₄. ¹H NMR ([D₅]py, 23 °C): $\delta = 7.84$ (s, 10 H; BPh₄), 7.13 (s, 10 H; BPh₄), 5.74 (t, $J = 7$ Hz, 1 H; terpy), 5.70 (t, $J = 7$ Hz, 2 H; terpy), 4.37 (s, 30 H; Cp*), 3.79 (s, 2 H; terpy), 3.73 (s, 2 H; terpy), 2.78 (d, $J = 7$ Hz, 2 H; terpy), −16.50 ppm (s, 2 H; terpy).

Synthesis of [U(Cp*)₂{NC₅H₄(py)₂}][BPh₄] (6′): A flask was charged with **4b** (133 mg, 0.153 mmol) and NEt₃HBPh₄ (64 mg, 0.153 mmol), and THF (12 mL) was condensed into it. The reaction mixture was stirred at 20 °C for 12 h. The solvent was evaporated off, and the dark brown powder of **6′** was washed with toluene (15 mL) and dried under vacuum (131 mg, 81 %). ¹H NMR ([D₅]py, 23 °C): $\delta = 60.26$ (s, 2 H; N ligand), 16.19 (s, 30 H; Cp*), 7.31 (s, 10 H; Ph), 6.75 (s, 10 H; Ph), −0.10 (d, $J = 10$ Hz, 2 H; N ligand), −11.05 (d, $J = 10$ Hz, 2 H; N ligand), −19.29 (s, 2 H; N ligand), −19.43 (s, 2 H; N ligand), −114.27 ppm (s, 2 H; N ligand); elemental analysis calcd (%) for C₅₉H₆₂BN₃U (1062): C 66.73, H 5.88, N 3.96; found: C 66.51, H 5.72, N 4.10.

Table 4. Crystal data and structure refinement details.

	1a	**1b**	**3a·THF**	**3b·THF**	**4b**
empirical formula	$C_{30}H_{38}CeIN_2$	$C_{30}H_{38}IN_2U$	$C_{39}H_{49}CeIN_3O$	$C_{39}H_{49}IN_3OU$	$C_{35}H_{41}N_3U$
M [g mol⁻¹]	693.64	791.55	842.83	940.74	741.74
crystal system	monoclinic	monoclinic	monoclinic	trigonal	monoclinic
space group	$P2_1/c$	$P2_1/n$	$C2/c$	$R\bar{3}c$	$P2_1/n$
a [Å]	10.5719(12)	11.7734(4)	21.3196(9)	20.4936(8)	10.5915(5)
b [Å]	14.5662(16)	15.5242(5)	19.1336(10)	20.4936(8)	16.2320(11)
c [Å]	18.2757(15)	15.0045(5)	19.1138(8)	44.5824(12)	16.9469(11)
α [°]	90	90	90	90	90
β [°]	90.333(7)	94.699(2)	102.269(3)	90	91.731(4)
γ [°]	90	90	90	120	90
V [Å³]	2814.3(5)	2733.19(16)	7618.8(6)	16215.5(10)	2912.2(3)
Z	4	4	8	18	4
ρ_{calcd} [g cm⁻³]	1.637	1.924	1.470	1.734	1.692
$\mu(Mo_{K\alpha})$ [mm⁻¹]	2.734	7.089	2.037	5.395	5.602
$F(000)$	1372	1508	3384	8226	1456
data collected	18659	18544	25039	35292	19885
unique data	5302	5150	7003	3420	5252
observed data $[I > 2\sigma(I)]$	3828	4339	5084	2930	4120
R_{int}	0.112	0.066	0.104	0.086	0.070
parameters	317	317	416	234	352
R_1	0.053	0.033	0.073	0.029	0.033
wR_2	0.107	0.072	0.171	0.058	0.071
S	1.057	1.047	1.012	1.072	1.037
$\Delta\rho_{min}$ [e Å⁻³]	−1.48	−0.72	−1.74	−0.67	−0.66
$\Delta\rho_{max}$ [e Å⁻³]	0.71	0.71	1.34	0.64	0.55

	5b·toluene	**6·py**	**6′**	**7**
empirical formula	$C_{62}H_{79}I_2N_3U_2$	$C_{40}H_{47}IN_4U$	$C_{59}H_{64}BN_3U$	$C_{35}H_{46}IN_3U$
M [g mol⁻¹]	1596.14	948.75	1061.96	873.68
crystal system	monoclinic	trigonal	monoclinic	orthorhombic
space group	Cc	$R\bar{3}$	$P2_1/n$	$Pbca$
a [Å]	26.2124(8)	27.3459(6)	10.2979(11)	15.844(2)
b [Å]	16.7828(7)	27.3459(6)	32.855(3)	22.054(3)
c [Å]	16.2870(7)	26.0915(10)	14.0282(13)	18.2807(12)
α [°]	90	90	90	90
β [°]	125.122(2)	90	92.230(7)	90
γ [°]	90	120	90	90
V [Å³]	5860.4(4)	16897.2(8)	4742.7(8)	6387.7(13)
Z	4	18	4	8
ρ_{calcd} [g cm⁻³]	1.809	1.678	1.487	1.817
$\mu(Mo_{K\alpha})$ [mm⁻¹]	6.613	5.177	3.465	6.077
$F(000)$	3048	8280	2136	3376
data collected	19621	38548	25853	50728
unique data	10490	7047	8644	6006
observed data $[I > 2\sigma(I)]$	9763	5525	6119	4061
R_{int}	0.055	0.101	0.091	0.074
parameters	632	428	587	381
R_1	0.043	0.052	0.058	0.052
wR_2	0.099	0.105	0.137	0.097
S	1.036	1.065	1.052	1.051
$\Delta\rho_{min}$ [e Å⁻³]	−1.46	−1.18	−1.19	−1.35
$\Delta\rho_{max}$ [e Å⁻³]	1.04	1.64	1.77	0.75

Reaction of 5b with Ph₃SnH: An NMR tube was charged with **5b** (24.8 mg, 0.016 mmol) and Ph₃SnH (15.0 mg, 0.042 mmol) in THF (0.4 mL). The tube was stirred for 18 h at 20 °C; the solvent was evaporated off and replaced with [D₅]py. The spectrum of the dark green solution showed the formation of [U(Cp*)₂I(py)] (50 %), **6** (20 %), **7** (18 %) and an unidentified product (12 %) with a Cp* signal at $\delta = 16.16$ ppm.

Reaction of 5b with NEt₃HBPh₄: An NMR tube was charged with **5b** (18.9 mg, 0.011 mmol) and NEt₃HBPh₄ (4.8 mg, 0.011 mmol) in [D₈]THF. The tube was immersed in the ultrasound bath for 15 min. The color of the solution turned from green to orange, and the spectrum showed the formation of an equimolar mixture of **6′** and [U(Cp*)₂I₂].

Reaction of 6′ with Na(Hg): An NMR tube was charged with **6** (18.4 mg, 0.017 mmol) and 2 % Na(Hg) (60 mg, 0.052 mmol of Na) in [D₈]THF (0.4 mL). The tube was immersed in the ultrasound bath for 2 h. The color of the solution turned from orange to green, and the spectrum showed almost quantitative formation of **4b**.

Synthesis of [U(Cp*)₂{NC₅H₈(py)₂}]I (7): A flask was charged with **3b** (160 mg, 0.184 mmol) and Ph₃SnH (342 mg, 0.975 mmol), and pyridine (12 mL) was condensed into it. The reaction mixture was heated at 120 °C for 8 h. The solvent was evaporated off and the orange powder of **7** was washed with THF (15 mL) and dried under vacuum (96.4 mg, 68 %). ¹H NMR ([D₅]py, 23 °C): $\delta = 78.06$ (d, $J = 12$ Hz, 2 H; N ligand), 12.60 (br, 1 H; N ligand), 11.81 (s, 15 H; Cp*), 11.56 (br, 1 H; N ligand), 10.30 (s, 15 H; Cp*), 4.28 (dd, $J = 12$ Hz, 2 H; N ligand), 3.74 (t, $J = 10$ Hz, 2 H; N ligand), 1.79 (d, $J = 10$ Hz, 2 H; N ligand), 0.45 (d, $J = 10$ Hz, 2 H; N ligand), −18.58 (br s, 2 H; N ligand), −95.69 ppm (br s, 2 H; N ligand); elemental analyses calcd (%) for C₃₅H₄₆IN₃U (873.7): C 48.12, H 5.31, N 4.81; found: C 48.05, H 5.40, N 4.80.

Crystal structure determinations: Data were collected at 100(2) K on a Nonius Kappa-CCD area detector diffractometer[41] using graphite-monochromated Mo$_{K\alpha}$ radiation ($\lambda = 0.71073$ Å). The crystals were introduced into glass capillaries with a protecting Paratone-N oil (Hampton Research) coating. The unit-cell parameters were determined from ten frames, then refined on all data. The data (Φ scans) were processed with DENZO-SMN.[42] The structures were solved by Patterson map interpretation (**6′**) or by direct methods (all other compounds) with SHELXS-97 and subsequent Fourier-difference synthesis and refined by full-matrix least-squares techniques on F^2 with SHELXL-97.[43] Absorption effects were corrected empirically with the program DELABS from PLATON.[44] In all compounds, all non-hydrogen atoms were refined with anisotropic displacement parameters. In compounds **3a**·THF, **3b**·THF, **5b**·toluene, **6**·py and **6′**, some restraints on bond displacements had to be applied for some badly behaving atoms, particularly in some Cp* moieties, the solvent molecules and one aromatic ring of the BPh₄ group in **6′**, possibly indicating the presence of unresolved disorder in some cases. Restraints on bond lengths were also applied for the tetrahydrofuran molecule in **3b**·THF, which is disordered over two positions with 0.5 occupancy factor, and the aromatic ring of the toluene molecule in **5b**·toluene was refined as an idealized hexagon. Some voids in the structure of **6**·py, as well as the highest residual electron density peak located on the threefold axis, likely indicate the presence of another, unresolved solvent molecule. The iodine atom in **7** is disordered over two positions with refined occupancy parameters of 0.87(2) and 0.13(2); the latter position, which was somewhat unstable, was refined with restraints on displacement parameters. The hydrogen atoms were introduced at calculated positions in all compounds (except for the disordered tetrahydrofuran molecule in **3b**·THF) and were treated as riding atoms with a displacement parameter equal to 1.2 (CH, CH₂) or 1.5 (CH₃) times that of the parent atom. The absolute structure in **5b**·toluene was determined from the value of the Flack parameter (0.004(6).[45] Crystal data and structure refinement details are given in Table 4. The molecular plots were drawn with SHELXTL.[46]

CCDC-270339–CCDC-270347 contain the supplementary crystallographic data for this paper. These data can be obtained free of charge from the Cambridge Crystallographic Data Centre via www.ccdc.cam.ac.uk/data_request/cif.

[1] a) C. J. Burns, B. E. Bursten, *Comments Inorg. Chem.* **1989**, *9*, 61–93; b) B. E. Bursten, L. F. Rhodes, R. J. Strittmatter, *J. Am. Chem. Soc.* **1989**, *111*, 2756–2758; c) M. Mazzanti, R. L. Wietzke, J. Pecaut, J. M. Latour, P. Maldivi, M. Remy, *Inorg. Chem.* **2002**, *41*, 2389–2399; d) N. Kaltsoyannis, *Chem. Soc. Rev.* **2003**, *32*, 9–16; e) D. Guillaumont, *J. Phys. Chem. A* **2004**, *108*, 6893–6900.

[2] a) K. L. Nash, *Solvent Extr. Ion Exch.* **1993**, *11*, 729–768; b) K. L. Nash in *Handbook on the Physics and Chemistry of Rare Earths. Lanthanides/Actinides: Chemistry* (Ed.: K. A. Gschneidner, Jr., L. Eyring, G. R. Choppin, G. H. Lander), Elsevier Science, Amsterdam, **1994**, vol. 18, p. 197; c) *Actinides and Fission Products Partitioning and Transmutation. Status and Assessment Report*, NEA/OECD Report, NEA/OECD, Paris, **1999**; d) *Actinides and Fission Products Partitioning and Transmutation*, Proceedings of the Fifth International Information Exchange Meeting, Mol, Belgium, 25–27 Nov 1998, NEA/OECD Report, Paris, **1999**.

[3] C. Rivière, M. Nierlich, M. Ephritikhine, C. Madic, *Inorg. Chem.* **2001**, *40*, 4428–4435.

[4] J. C. Berthet, C. Rivière, Y. Miquel, M. Nierlich, C. Madic, M. Ephritikhine, *Eur. J. Inorg. Chem.* **2002**, 1439–1446.

[5] J. C. Berthet, Y. Miquel, P. B. Iveson, M. Nierlich, P. Thuéry, C. Madic, M. Ephritikhine, *J. Chem. Soc. Dalton Trans.* **2002**, 3265–3272.

[6] J. C. Berthet, M. Nierlich, Y. Miquel, C. Madic, M. Ephritikhine, *Dalton Trans.* **2005**, 369–379.

[7] a) S. Colette, B. Amekraz, C. Madic, L. Berthon, G. Cote, C. Moulin, *Inorg. Chem.* **2002**, *41*, 7031–7041; b) L. Karmazin, M. Mazzanti, J. P. Bezombes, C. Gateau, J. Pécaut, *Inorg. Chem.* **2004**, *43*, 5147–5158.

[8] D. J. Berg, J. M. Boncella, R. A. Andersen, *Organometallics* **2002**, *21*, 4622–4631.

[9] W. J. Evans, D. K. Drummond, *J. Am. Chem. Soc.* **1989**, *111*, 3329–3335.

[10] M. Schultz, J. M. Boncella, D. J. Berg, T. Don Tilley, R. A. Andersen, *Organometallics* **2002**, *21*, 460–472.

[11] R. E. Da Re, C. J. Kuehl, M. G. Brown, R. C. Rocha, E. D. Bauer, K. D. John, D. E. Morris, A. P. Shreve, J. L. Sarrao, *Inorg. Chem.* **2003**, *42*, 5551–5559.

[12] C. J. Kuehl, R. E. Da Re, B. L. Scott, D. E. Morris, K. D. John, *Chem. Commun.* **2003**, 2336–2337.

[13] a) F. G. N. Cloke, H. C. de Lemos, A. A. Sameh, *J. Chem. Soc. Chem. Commun.* **1986**, 1344–1345; b) M. N. Bochkarev, A. A. Trifonov, F. G. N. Cloke, C. L. Dalby, P. T. Matsunaga, R. A. Andersen, H. Schumann, J. Loebel, H. Hemling, *J. Organomet. Chem.* **1995**, *486*, 177–182; c) H. Sugiyama, I. Korobkov, S. Gambarotta, A. Miller, P. H. M. Budzelaar, *Inorg. Chem.* **2004**, *43*, 5771–5779.

[14] G. Del Piero, G. Perego, A. Zazzetta, G. Brandi, *Cryst. Struct. Comm.* **1975**, *4*, 521–527.

[15] A. R. Shake, L. R. Avens, C. J. Burns, D. L. Clark, A. P. Sattelberger, W. H. Smith, *Organometallics* **1993**, *12*, 1497–1498.

[16] T. Mehdoui, J. C. Berthet, P. Thuéry, M. Ephritikhine, *Dalton Trans.* **2004**, 579–590.

[17] T. Mehdoui, J. C. Berthet, P. Thuéry, M. Ephritikhine, *Eur. J. Inorg. Chem.* **2004**, 1996–2000.

[18] J. C. Berthet, J. M. Onno, C. Rivière, M. Nierlich, M. Ephritikhine, C. Madic, Poster presented at the 23rd Rare Earth Research Conference, Davis, USA, July **2002**.

[19] a) R. S. Sternal, M. Sabat, T. J. Marks, *J. Am. Chem. Soc.* **1987**, *109*, 7920–7921; b) Z. Lin, J. F. Le Maréchal, M. Sabat, T. J. Marks, *J. Am. Chem. Soc.* **1987**, *109*, 4127–4129.

[20] R. D. Shannon, *Acta Crystallogr. Sect. A* **1976**, *32*, 751–767.

[21] I. L. Fedushkin, T. V. Petrovskaya, F. Girgsdies, R. D. Köhn, M. N. Bochkarev, H. Schumann, *Angew. Chem.* **1999**, *111*, 2407–2409; *Angew. Chem. Int. Ed.* **1999**, *38*, 2262–2267.

[22] M. H. Chisholm, J. C. Huffman, I. P. Rothwell, P. G. Bradley, N. Kress, W. H. Woodruff, *J. Am. Chem. Soc.* **1981**, *103*, 4945–4947.

[23] J. C. Berthet, M. Ephritikhine, *Coord. Chem. Rev.* **1998**, *178–180*, 83–116.

[24] C. Boisson, J. C. Berthet, M. Lance, M. Nierlich, M. Ephritikhine, *J. Organomet. Chem.* **1997**, *548*, 9–16.

[25] T. Straub, W. Frank, G. J. Reiss, M. Eisen, *J. Chem. Soc. Dalton Trans.* **1996**, 2541–2546.

[26] C. A. Bessel, R. F. See, D. L. Jameson, M. Rowen Churchill, K. J. Takeuchi, *J. Chem. Soc. Dalton Trans.* **1992**, 3223–3228.

[27] L. Prasad, F. L. Lee, Y. Le Page, F. E. Smith, *Acta Crystallogr. Sect. B* **1982**, *38*, 259–262.

[28] J. C. Berthet, M. Nierlich, M. Ephritikhine, *Dalton Trans.* **2004**, 2814–2821.

[29] a) M. G. Hill, J. A. Bailey, V. M. Miskowski, H. B. Gray, *Inorg. Chem.* **1996**, *35*, 4585–4590; b) V. W. W. Yam, R. P. L. Tang, K. M. C. Wong, K. K. Cheung, *Organometallics* **2001**, *20*, 4476–4482; c) K. M. C. Wong, W. S. Tang, B. W. K. Chu, N. Zhu, V. W. W. Yam, *Organometallics* **2004**, *23*, 3459–3465.

[30] L. R. Avens, S. G. Bott, D. L. Clark, A. P. Sattelberger, J. G. Watkin, B. D. Zwick, *Inorg. Chem.* **1994**, *33*, 2248–2256.

[31] a) J. C. Berthet, P. Thuéry, M. Ephritikhine, *Inorg. Chem.* **2005**, *44*, 1142–1146; b) U. Casellato, R. Graziani, *Z. Kristallogr. New Cryst. Struct.* **1998**, *213*, 361–362; c) J. Rebizant, M. R. Spirlet, G. Van Den Bossche, J. Goffart, *Acta Crystallogr. Sect. C* **1988**, *44*, 1710–1712; d) J. H. Levy, J. C. Taylor, A. B. Waugh, *Inorg. Chem.* **1980**, *19*, 672–674; e) J. C. Taylor, *Coord. Chem. Rev.* **1976**, *20*, 197–273.

[32] M. L. Kahn, J. P. Sutter, S. Golhen, P. Guionneau, L. Ouahab, O. Kahn, D. Chasseau, *J. Am. Chem. Soc.* **2000**, *122*, 3413–3421.

[33] M. L. Kahn, C. Mathoniere, O. Kahn, *Inorg. Chem.* **1999**, *38*, 3692–3697.

[34] J. P. Costes, F. Dahan, A. Dupuis, J. P. Laurent, *Chem. Eur. J.* **1998**, *4*, 1616–1620.

[35] a) A. Figuerola, C. Diaz, J. Ribas, V. Tangoulis, J. Granell, F. Lloret, J. Mahia, M. Maestro, *Inorg. Chem.* **2003**, *42*, 641–649; b) Y. Zou, W. L. Liu, S. Gao, C. S. Lu, D. B. Dang, Q. J. Meng, *Polyhedron* **2004**, *23*, 2253–2258; c) T. Shiga, M. Ohba, H. Okawa, *Inorg. Chem.* **2004**, *43*, 4435–4446; d) J. P. Costes, F. Dahan, G. Novitchi, V. Arion, S. Shova, J. Lipkowski, *Eur. J. Inorg. Chem.* **2004**, 1530–1537.

[36] B. Kanellakopulos in *Organometallics of the f Elements* (Eds.: T. J. Marks, R. D. Fischer), Reidel, Dordrecht, **1979**, pp. 1–35.

[37] J. A. Joule, G. F. Smith, *Heterocyclic Chemistry*, Van Nostrand Reinhold, London, **1972**, chap. 4, and references therein.

[38] a) W. J. Evans, J. H. Meadows, W. E. Hunter, J. L. Atwood, *J. Am. Chem. Soc.* **1984**, *106*, 1291–1300; b) B. J. Deelman, W. M. Stevels, J. H. Teuben, M. T. Lakin, A. L. Spek, *Organometallics* **1994**, *13*, 3881–3891; c) R. Duchateau, C. T. van Wee, J. H. Teuben, *Organometallics* **1996**, *15*, 2291–2302; d) E. Kirillov, C. W. Lehmann, A. Razavi, J. F. Carpentier, *Eur. J. Inorg. Chem.* **2004**, 943–945.

[39] a) T. Le Borgne, E. Rivière, J. Marrot, P. Thuéry, J. J. Girerd, M. Ephritikhine, *Chem. Eur. J.* **2002**, *8*, 773–783; b) L. Salmon, P. Thuéry, E. Rivière, J. J. Girerd, M. Ephritikhine, *Dalton Trans.* **2003**, 2872–2880.

[40] L. R. Avens, C. J. Burns, R. J. Butcher, D. L. Clark, J. C. Gordon, A. R. Schake, B. L. Scott, J. G. Watkin, B. D. Zwick, *Organometallics* **2000**, *19*, 451–457.

[41] Kappa-CCD Software, Nonius B.V., Delft, **1998**.

[42] Z. Otwinowski, W. Minor, *Methods Enzymol.* **1997**, *276*, 307–326.

[43] G. M. Sheldrick, SHELXS-97 and SHELXL-97, University of Göttingen, **1997**.

[44] A. L. Spek, PLATON, University of Utrecht, **2000**.

[45] H. D. Flack, *Acta Crystallogr. Sect. A* **1983**, *39*, 876–881.

[46] G. M. Sheldrick, SHELXTL, Version 5.1, Bruker AXS Inc., Madison, WI, **1999**.